

1 **Short title:** Side-chain motion of partially non-crystallized wood

2

3 **Title:** Side-chain motion of components in wood samples partially non-crystallized using

4 NaOH-water solution

5

6 **Authors:** Takashi Tanimoto<sup>1</sup> and Takato Nakano<sup>2\*</sup>

7

8 **Author affiliations:**

9 1: ASAHI WOODTECH COMPANY, Chuoh-ku, Osaka, 541-0054, Japan

10 2: Laboratory of Biomaterials Design, Division of Forest and Biomaterials Science, Graduate School

11 of Agriculture, Kyoto University, Kita-Shirakawa, Kyoto, 606-8502 Japan

12

13 **\*: corresponding author**

14 Laboratory of Biomaterials Design, Division of Forest and Biomaterials Science, Graduate School of

15 Agriculture, Kyoto University, Kita-Shirakawa, Kyoto, 606-8502 Japan

16 Tel.:+81-75-753-6234

17 .e-mail address: [tnakano@kais.kyoto-u.ac.jp](mailto:tnakano@kais.kyoto-u.ac.jp).

18 **Abstract**

19 Wood samples (*Picea jezoensis* Carr.) were treated with solutions of aqueous NaOH (0–0.20  
20 concentration fraction) and each treated samples evaluated by dynamic mechanical analyses (DMA).  
21 NaOH treatment was shown to affect the interactions between microfibrils and the surrounding  
22 matrix and, in particular, the dynamics of methylol groups in the microfibrils. The former is not  
23 dependent on the degree of crystallization but rather on the eluviation of the matrix. The latter  
24 depends on the degree of crystallization. Alkali treatment induces changes in the polymer  
25 domains as a result of matrix eluviation. This decreases the dynamics of methylol groups at NaOH  
26 concentrations less than 0.11. On the other hand, alkali treatment causes non-crystallization at  
27 concentrations greater than 0.11, which quantitatively increases the flexibility of methylol groups.  
28 Crystallinity decreased, and main-chain dynamics increased, following treatment with highly  
29 concentrated NaOH solutions. The dynamics of lignin also increased due to weakened interactions  
30 with microfibrils due to non-crystallization.

31

32 **Keywords:** Side-chain, NaOH treatment, Viscoelasticity, Microfibril, Crystallinity

33

34 **1. Introduction**

35 Native cellulose can be transformed into other crystalline forms via NaOH-water treatment [1-6]. In  
36 plant cell walls such as wood, native cellulose is mostly found as microfibrils of cellulose aggregate  
37 with high crystallinity, which contains two crystalline forms, Ia and Ib. Recently, the dissolution  
38 mechanism of cellulose with NaOH treatment has been reported based on results by various  
39 methods. Roy et al. [7] proposed a mechanism for lower temperatures. Cai et al. [8-10] applied the  
40 method of Navard et al. [11] to the NaOH/urea system. Additionally, the alkali treatment is applied  
41 to various composites in practice and their physical properties are examined [12-15].

42 This paper discusses the molecular dynamics, especially side-chain motion, of wood components  
43 in wood cells that have been non-crystallized by alkali treatment. Nakano [16] reported that wood  
44 contracts drastically along its longitudinal axis and demonstrated that this contraction is due to an  
45 entropic elastic force caused by the non-crystallization of cellulose microfibrils [17]. Anisotropic  
46 dimensional changes have been reported during alkali treatment [18]. Nakano [19] examined this  
47 anisotropy based on model analysis.

48 Changes in dynamics of wood sample during non-crystallization were reported in an analysis of  
49 the NaOH concentration ([NaOH]) dependence on stress relaxation [20]. The relaxation modulus  
50 and relaxation rate of them were divided into three concentration ranges: less than [NaOH] = 0.10,  
51 between 0.11 and 0.14, and greater than 0.15. Changes in relaxation dynamics were due to  
52 increases in molecular chain mobility in non-crystallized regions along the longitudinal axis of

53 microfibrils in wood and to lignin swelling as a result of NaOH treatment. That is, the dependence  
54 of crystallinity on the relaxation time was related to molecular chain rearrangements required time  
55 in this region.

56 This study focuses on changes in non-crystallized cellulose chain dynamics and on the  
57 concentration (crystallization) dependence of dynamic viscoelastic behavior, especially side-chain  
58 motion. The domains of the cellulose chain and the interactions between cellulose and other wood  
59 components are discussed.

60

## 61 **2. Experimental**

### 62 **2.1. Materials and NaOH treatment**

63 Wood specimens of 70 (L) × 7.5 (R) × 2 (T) mm were cut from Yezo spruce (*Picea jezoensis Carr.*): L,  
64 R, and T are longitudinal, radial, and tangential directions of wood, respectively. The samples were  
65 oven-dried at 70°C under vacuum with P<sub>2</sub>O<sub>5</sub> overnight. They were then soaked in aqueous NaOH  
66 with various concentrations ([NaOH] = 0 to 0.20) for 30 min and stored at room temperature for 2  
67 days. The samples were then washed in distilled water for 2 weeks. Washed samples were flash  
68 frozen in liquid N<sub>2</sub> and freeze-dried under vacuum for 1 day. The weight and dimensions of the dried  
69 samples were measured prior to dynamic mechanical analyses (DMA) and X-ray diffraction  
70 measurements.

71

72

## 73 **2.2. Dynamic mechanical analyses and X-ray diffraction measurements**

74 DMA measurements were acquired in dried-air with a dynamic mechanical analyzer DMA50  
75 (METRAVIB). In the chamber of DMA, dried-air was flowed before measurement. The moisture  
76 content of the samples was confirmed to be negligible small for each measurement. The  
77 measurement was performed with 5  $\mu\text{m}$  of tensile forced oscillation over a 40-mm span from  $-150$  to  
78  $200^\circ\text{C}$  at 1 Hz. The programmed heating rate was  $3^\circ\text{C}/\text{min}$ .

79 Crystallinity measurements were performed with an X-ray diffractometer RINT-UltimaIV  
80 (Rigaku). Diffractograms were obtained for the LR-plane at room temperature over a range of  $5$ – $35^\circ$ .  
81 The measurements were performed at 40 kV and 40 mA at a scan rate of  $2^\circ/\text{min}$ . The relative  
82 crystallinity of the samples was calculated as the ratio between the area of the crystalline  
83 contribution and the total area in the range of  $10$ – $28^\circ$ .

84

## 85 **3. Results and Discussion**

### 86 **3.1. Relative crystallinity and dimensional changes**

87 **Figures 1 and 2** shows the changes in dimension along the longitudinal direction of wood sample  
88 and relative crystallinity observed during NaOH treatment. Wood sample length characteristically  
89 decreased with increasing in NaOH concentration. The relative crystallinity was nearly constant for  
90 less than  $[\text{NaOH}] = 0.10$  but started to decrease at 0.11. Crystallinity decreased drastically between

91 [NaOH] = 0.11 and 0.13 and slightly for concentrations greater than 0.14. The  
92 concentration-dependence of dimensional changes along the longitudinal direction of each sample  
93 were similar to that of the crystallinity change. This indicates that the dimensional changes were  
94 due to non-crystallization with NaOH treatment. **Figure 2** suggests a linear relationship between  
95 both of these variables for concentrations greater than 0.11. These changes during NaOH treatment  
96 are consistent with our previous reports and indicate satisfactorily non-crystallization.

97

### 98 **3.2. Changes in molecular dynamics of non-crystallized wood**

99 **Figure 3(b)** shows the variation of  $\tan\delta$  as a function of temperature for treatments with [NaOH]=0  
100 and 0.20. Three characteristic relaxations were identified in the untreated ([NaOH] = 0) sample.  
101 These relaxations were labeled  $\alpha$ ,  $\beta$ , and  $\gamma$  in the order of decreasing temperature. The  $\beta$  relaxation  
102 was obscured in the fully dried samples. The  $\alpha$  dispersion was attributed to micro-Brownian motion  
103 of the cell wall polymers in the non-crystallized regions, the  $\beta$  dispersion was attributed to the  
104 motion of the absorbed water itself or the segmental motions associated with it, and the  $\gamma$  dispersion  
105 was attributed to the motion of methylol groups according to a previous study [21], [22]. These three  
106 relaxations of the untreated sample were identified at roughly the same temperatures for a sample  
107 treated with [NaOH] = 0.20. Therefore, the relaxations in the sample that had been treated with  
108 [NaOH] = 0.20 were attributed to the same causes as those in the untreated sample. However, their  
109 intensities and temperatures of  $\tan\delta$  have the characteristic concentration-dependence of NaOH

110 solution.

111 The temperature dependence of  $\tan\delta$  in the untreated sample was generally similar to that of  
112 the treated wood studied by other researchers and cellulose filaments [23]. However,  $\tan\delta$  intensity  
113 of both the  $\alpha$  and  $\gamma$  relaxations in samples that had been treated with NaOH 0.20 were much higher  
114 than those of the untreated sample.

115 The cause of the  $\beta$  relaxation has been discussed in several independent studies. Obataya *et al.*  
116 [22] assigned this relaxation to the absorbed water itself. Montés *et al.* [24] acquired DMA data on  
117 amorphous cellulose and other polysaccharides and reported that the  $\beta$  relaxation had a moisture  
118 dependence. In the current study, the  $\beta$  relaxation was indistinct in fully dried samples, which  
119 confirms a relationship to absorbed water but not to the absorbed water itself. The  $\alpha$  and  $\gamma$   
120 relaxations, which were observed in the current study, are discussed below.

121 **Figure 4** shows detailed profiles of  $\tan\delta$  of  $\gamma$  relaxation and exhibits characteristic changes in  
122 peak location and intensity during NaOH treatment. **Figures 5(a) and (b)** shows the peak intensity  
123 and location of  $\tan\delta$  for  $\gamma$  relaxation during NaOH treatments. Its dependence on NaOH  
124 concentration can be divided into three distinct ranges.  $\tan\delta$  was nearly constant for NaOH  
125 concentrations between  $[\text{NaOH}] = 0.00$  and  $0.10$ , then increased considerably between  $0.10$  and  $0.14$ ,  
126 and maintained a nearly constant value at NaOH concentrations greater than  $0.15$ . The peak  
127 shifted to a higher temperature range in the region below  $[\text{NaOH}] = 0.10$  and remained constant  
128 above  $[\text{NaOH}] = 0.11$ .

129 Side-chain relaxation generally depends on the dynamics of localized regions of molecular  
130 chains. Nakano [21] and Nakano et al. [25, 26] performed DMA on chemically modified wood,  
131 introducing various lengths of acyl groups, and reported that the dispersions assigned to side-chain  
132 motion depended on both the interactions between the side chains and the free volume created by  
133 the introduction of the acyl groups into wood substance. In the previous report, it was demonstrated  
134 that side-chain dispersion depends characteristically on the number of methylene group carbon.  
135 This result agrees with similar results obtained with PMMA [27]. While side-chain dynamics  
136 increases with increasing side-chain length for short side chains, it decreases in motion due to  
137 self-entanglement occurred for chain lengths more than 5 or 6 carbon atoms. Additionally, as for  
138 wood sample introduced dissociative side chains, the side-chain motion changes drastically by  
139 cross-linking with a metal ion [28, 29]. Considering these results in the previous work, changes in  
140 the intensity and location of the  $\gamma$  relaxation in the current study, which is due to the motion of side  
141 chains, also reflect changes in the methylol group domains during NaOH treatment.

142 The  $\alpha$  dispersion in wood is assigned to micro-Brownian motion in non-crystalline regions of  
143 wood components [30], which is influenced by environmental condition. For example, the  $\alpha$   
144 dispersion shifts to lower temperatures with increasing moisture content and shows a clear peak  
145 below 100°C at high moisture content [31, 32]. The moisture dependence on peak location roughly  
146 corresponds with that of the glass transition temperature ( $T_g$ ) of isolated lignin [32-34]. The  $\alpha$   
147 dispersion in the current study appeared as a shoulder. Thus, as the NaOH concentration



148 dependence on the  $\alpha$  peak location cannot be addressed here, the intensity of  $\tan\delta$  at 200°C, which is  
149 used as  $\tan\delta(200^\circ\text{C})$ , is discussed in the following discussion. **Figure 6** shows the relationship  
150 between  $\alpha$  intensity and NaOH concentration.  $\tan\delta(200^\circ\text{C})$  was nearly constant for concentrations  
151 less than NaOH 0.10 and increased at concentrations greater than 0.11. This result clearly  
152 corresponds to that shown in Figure 1.

153

### 154 3.3. Changes in storage modulus

155 **Figure 3(a)** shows the variation in relative storage modulus, normalized to  $-120^\circ\text{C}$ . The storage  
156 modulus was nearly constant for NaOH concentrations less than  $[\text{NaOH}] = 0.10$  and showed a  
157 characteristic decrease at concentrations greater than 0.11. Changes in storage modulus at greater  
158 than  $[\text{NaOH}] = 0.11$  were composed of two processes. The first process caused a slight decrease  
159 between  $-120$  and  $-70^\circ\text{C}$ ; the other process resulted in a drastic decrease above  $100^\circ\text{C}$ . The former  
160 and latter correspond to changes in the  $\gamma$  dispersion, as shown in **Figure 4** and in the  $\alpha$  dispersion  
161 shown in **Figure 3(b)**, respectively.

162 **Figure 7** shows the concentration dependence on relative modulus at  $-70$ ,  $100$ , and  $200^\circ\text{C}$ . At all  
163 temperatures, the relative modulus decreased drastically at concentration 0.10. The decrease at  
164  $-70^\circ\text{C}$  was less than that at the other two temperatures. However, a clear decrease was observed at  
165 concentrations greater than 0.11. The observed decrease in relative modulus was more clear at  
166  $200^\circ\text{C}$  than at  $100^\circ\text{C}$  at greater than  $[\text{NaOH}] = 0.11$ . This effect might be due to a glass transition in

167 dry lignin in this temperature region [35]. While the relative modulus at  $-70^{\circ}\text{C}$  is nearly constant at  
168 less than  $[\text{NaOH}] = 0.10$ , and then decreased at greater than  $[\text{NaOH}] = 0.10$ . This difference in  
169 temperature dependence of the storage modulus agrees with the concentration dependencies of  $\tan\delta$   
170 of the  $\alpha$  and  $\gamma$  dispersions.

171

### 172 3.4. Crystallinity dependence on $\gamma$ and $\alpha$ dispersions

173 The aforementioned characteristic concentration dependence on the  $\gamma$  dispersion is due to a change  
174 in methylol group domains, according to viscoelasticity measurements of chemically modified wood  
175 [21], [25, 26]. This concentration dependence may be discussed in terms of relative crystallinity.  
176 **Figures 8(a) and (b)** show the dependence of crystallinity on the  $\tan\delta$  intensity and the peak position  
177 of the  $\gamma$  dispersion, respectively. The  $\tan\delta$  increased slightly with near constant crystallinity at less  
178 than  $[\text{NaOH}] = 0.11$ . The trend then leveled off after a drastic increase with a decrease in  
179 crystallinity at greater than  $[\text{NaOH}] = 0.11$  (**Figure 8(a)**). The peak corresponding to the  $\gamma$   
180 dispersion shifted to higher temperatures with increasing NaOH concentration for samples with  
181 constant crystallinity at less than  $[\text{NaOH}] = 0.11$ , while it did not shift with a decrease in  
182 crystallinity at higher concentration (**Figure 8(b)**).

183 The data of the  $\gamma$  dispersion in **Figures 8(a) and (b)** imply a change in the methylol domains  
184 during NaOH treatment. An initial change of  $\tan\delta$  with almost constant crystallinity is not due to  
185 change in the microfibrils themselves, because the shift in peak position occurred with no changes

186 in crystallinity. NaOH treatment induces two changes in wood. The first is a structural change of  
187 cellulose, the main ingredient in wood, known as mercerization. The second is the eluviation of wood  
188 components. NaOH treatment eluviate hemicellulose and some lignin [36-38]. Therefore, it may be  
189 inferred that a change occurring at constant crystallinity is due to this eluviation. An average  
190 weight loss of approximately 6% was observed in samples treated with NaOH at the concentrations  
191 used in this study.

192 Furthermore, it may be inferred that the methylol domains experienced restricted flexibility as  
193 they approached each other as a result of hemicellulose eluviation and the partial eluviation of  
194 lignin. This decreased flexibility, in turn, resulted in a peak shift to higher temperatures and a  
195 decrease in  $\tan\delta$ . This restriction effect is manifested in the concentration dependence of the relative  
196 modulus at  $-70^{\circ}\text{C}$  in **Figure 6**. Relative modulus did not decrease but constant at less than  $[\text{NaOH}]$   
197  $= 0.10$  at this temperature, comparing with the other temperature.

198 The minimal crystallinity dependence of the  $\tan\delta$  peak position at greater than  $[\text{NaOH}] = 0.11$   
199 shown in **Figure 8(b)** indicates a negligible change in the flexibility of the methylol groups. Note,  
200 however, that  $\tan\delta$  increased with decreasing in crystallinity (**Figure 8(a)**), and the dispersion of the  
201 peak widened (**Figure 4**). This result strongly suggests an increase in the relative proportion of  
202 regions that contribute to the relaxation process. In other words, results of the  $\gamma$  dispersion shown in  
203 **Figures 8(a) and (b)** show that the relative number of methylol groups affecting relaxation increased  
204 due to an increase in amorphous domains. Nakano [21] pointed out that an increase in the amount

205 of side chains introduced during esterification caused an increase in the free volume. This increased  
206 the flexibility of both the side chains themselves and the main chains. However, the effect was  
207 smaller for shorter side chains. Additionally, effects due to hydrogen bonding with the hydroxyl  
208 group can be expected with methylol groups. Therefore, contributions restricting flexibility were  
209 larger at  $-70^{\circ}\text{C}$ , comparing with the other temperatures 100 and  $200^{\circ}\text{C}$  (**Figure 7**).

210 The  $\tan\delta$  at 100 and  $200^{\circ}\text{C}$  increase increased drastically between  $[\text{NaOH}] = 0$  and 0.12 and  
211 then gradually increased at greater than  $[\text{NaOH}] = 0.12$ . Considering that the  $\alpha$  dispersion is  
212 assigned to main-chain motion of lignin by which hemicellulose and cellulose microfibril surface are  
213 bonded, **Figure 9(a)** suggests that the interaction between the both is weakened by the eluviation of  
214 the matrix in wood with NaOH treatment.

215 The crystallinity dependence of the storage modulus shown in **Figure 9(b)** corresponds roughly  
216 with that of  $\tan\delta$  in **Figure 9(a)**. **Figure 9(b)** shows the dependence of the relative modulus on the  
217 degree of crystallinity at 100 and  $200^{\circ}\text{C}$ . The relative modulus decreased drastically between  
218  $[\text{NaOH}] = 0.11$  and 0.12, was nearly constant between 0.12 and 0.15, and then decreased again at  
219 greater than  $[\text{NaOH}] = 0.15$ . This dependence is similar to that of the relaxation modulus, which  
220 measures stress relaxation, in our previous study [20]. This is because a decrease in the storage  
221 modulus at high concentrations is related to the main chain and not to the dynamics of the side  
222 chains.

223

224 **4. Conclusions**

225 Changes in molecular dynamics in wood as the result of NaOH treatment were examined using  
226 DMA measurements. It was shown that NaOH treatment affects the interactions between  
227 microfibrils and the surrounding matrix and the dynamics of methylol groups in the microfibrils.  
228 The former is not dependent on the degree of crystallization but rather on the eluviation of the  
229 matrix. The latter depends on the degree of crystallization. Low-concentration NaOH treatment  
230 induces changes in the polymer domains through the eluviation of the matrix material. Conversely,  
231 at high alkali concentrations, the proportion of domains that are involved in methylol group  
232 dynamics increases quantitatively, indicating significant non-crystallization. In addition,  
233 main-chain dynamics in wood increased with decreasing crystallinity. The interactions between  
234 microfibrils and matrix are believed to be weakened by the swelling of matrix and the shrinkage of  
235 microfibrils, thereby increasing the flexibility of matrix.

236 **References**

- 237 [1] Revol, J.-F., Goring, D.A.I. *J. Appl. Polym. Sci.* **1978**, 16, 1275-1282.
- 238 [2] Murase, H., Sugiyama, J., daiki, H., Harada, H. *Mokuzai Gakkaishi* **1978**, 34, 965-972.
- 239 [3] Okano, T. and Sarko, A. *J. Appl. Polym.* **1984**, 29, 4175-4182
- 240 [4] Okano, T. and Sarko, A. *J. Appl. Polym.* **1985**, 30, 325-332.
- 241 [5] Nishimura, H., Okano, T., Sarko, A. *Macromolecules* **1991a**, 24, 759-770.
- 242 [6] Nishimura, H., Okano, T., Sarko, A. *Macromolecules* **1991b**, 24, 771-778.
- 243 [7] Roy, C., Budtova, T., Navard, P., Bedue, O. *Biomacromolecules* **2001**, 2, 687-693.
- 244 [8] Cai, J., Zhang, L. *Biomacromolecules* **2006**, 7, 183-189.
- 245 [9] Cai, J., Zhang, L., Chang, C., Cheng, G., Chen, X., Chu, B. *Chem. Phys. Chem.* **2007a**, 8,
- 246 1572-1579.
- 247 [10] Cai, J., Zhang, L., Zhou, J., Qi, H., Chen, H., Kondo, T., Chen, X., Chu, B. *Adv. Materials* **2007b**,
- 248 19, 821-825.
- 249 [11] Roy, C., Budtova, T, Navard, P., Bedue, O. *Biomacromolecules* **2001**, 2, 687-693.
- 250 [12] Yan, L, Chouw, N., Yuan, X. *J. Reinf. Plast.Comp.*, 31 (2012) 425.
- 251 [13] Li, L., Sun, J., Jia, G. *J. Appl. Polym. Sci.*, 125 (2012) E534.
- 252 [14] Ashori, A., Ornelas, M, Sheshmani, S., Cordeiro, N. *Carbohydrate Polymers*, 88 (2012) 1293.
- 253 [15] Mwaikambo, L.Y., Ansell, M.P. *J. Mater. Sci.* (2006) 2483.

254

- 255 [16] T. Nakano, Mokuzai Gakkaishi, 35, (1989) 431.
- 256 [17] T. Nakano, J. Sugiyama, M. Norimoto, Holzforschung, 54, (2000) 315.
- 257 [18] Y. Ishikura, T. Nakano, J. Wood Sci., 53, (2007) 175.
- 258 [19] T. Nakano, Cellulose, 17, (2010) 711.
- 259 [20] T. Tanimoto, T. Nakano, Carbohydrate Polymers, 87, (2011) 2145.
- 260 [21] T. Nakano, Holzforschung, 48, (1994) 318.
- 261 [22] E. Obataya, M. Norimoto, B. Tomita, B., J. Appl. Polym. Sci., 81, (2001) 3338.
- 262 [23] C. Yamane, M. Mori, M. Saito, K. Okajima, Polym. J., 28, (1996) 1039.
- 263 [24] H. Montés, K. Mazeran, J.Y. Cavaillé, Macromolecules, 30, (1997) 6977.
- 264 [25] T. Nakano, S. Honma, A. Matsumoto, Mokuzai Gakkaishi, 36, (1990) 1063.
- 265 [26] T. Nakano, S. Honma, A. Matsumoto, Mokuzai Gakkaishi, 37, (1991) 924.
- 266 [27] E.A.W. Hoff, D.W. Robinson, A.H. Willbourn, J. Polym. Sci., 18, (1955) 161.
- 267 [28] Nakano, T., Holzforschung, 47, (1993) 202.
- 268 [29] Nakano, T, Holzforschung, 47, (1993) 278.
- 269 [30] T. Sadoh, *Wood science and technology*, 15, (1981) 57.
- 270 [31] H. Becker, D. Noack, *Wood science and technology*, 2, (1968) 213.
- 271 [32] S.S. Kelley, T.G. Rials, W.G. Glasser, *J. materials science*, 22, (1987) 617.
- 272 [33] G.M. Irvin, G.M., Tappi J, 67, (1984) 118.
- 273 [34] L. Salmén, A.-M. Olsson, J. Pulp and Paper Sci., 24, (1998) 99.

274 [35] Goring, D.A.I. Pulp and Paper Magazine Canada, 64 (1963) T517.

275 [36] Hamiss, E.E., Ind. and Eng. Chem, 5, (1933) 105.

276 [37] Schuerch Jr., C, J. Am. Chem. Soc., 72, (1950) 3838.

277 [38] Bailey, R.W., Pickmere, S.E., 14, (1975) 501.

278



279 **Figure captions**

280 Figure 1. Dimensional changes under wet condition along the longitudinal axis of wood samples  
281 Yezo spruce (*Picea jezoensis Carr.*) as a function of NaOH concentration.

282

283 Figure 2. Crystallinity and relative dimensional changes along the longitudinal axis ( $\Delta L/L$ ) of wood  
284 samples as a function of NaOH concentration.

285

286 Figure 3. The typical temperature dispersion of the relative dynamic modulus normalized to its  
287 value at  $-120^{\circ}\text{C}$  (a) and  $\tan\delta$  (b) under dry condition for samples treated with various aqueous  
288 NaOH solutions.

289

290 Figure 4. The NaOH concentration dependence of  $\tan\delta$  assigned to methylol groups in wood for  
291 samples treated with NaOH treatment.

292

293 Figure 5. The NaOH concentration dependence of  $\tan\delta(\gamma)$  and temperature ( $T_{\gamma}$ ) of the  $\gamma$   
294 dispersion assigned to methylol groups.

295

296 Figure 6.  $\tan\delta$  intensity at  $200^{\circ}\text{C}$  as a function of NaOH concentration.

297

298 Figure 7. The relative dynamic modulus at various temperatures normalized to its value at 120°C

299 as a function of NaOH concentration.

300

301 Figure 8. The crystallinity dependence of the peak intensity and temperature of  $\tan\delta$  for methylol

302 groups in wood.

303

304 Figure 9. The crystallinity dependence of the  $\tan\delta$  intensity at 200°C and the relative dynamic

305 modulus at 100 and 200°C.

306

307

308

309

310

311

312

313

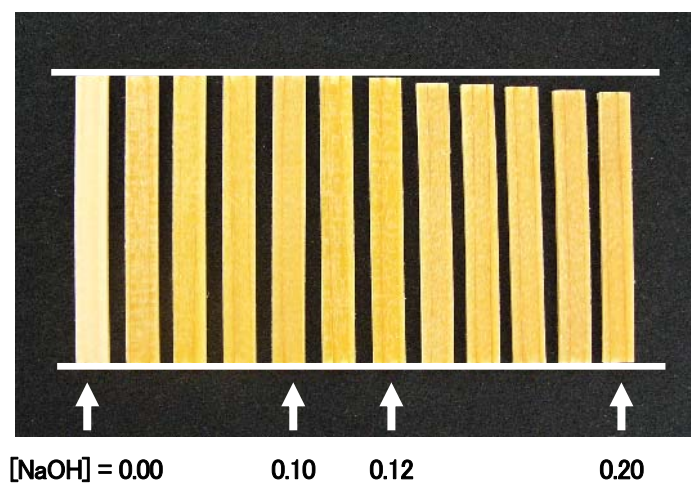
314

315

316

317

318



319 Figure 1

320

321

322

323

324

325

326

327

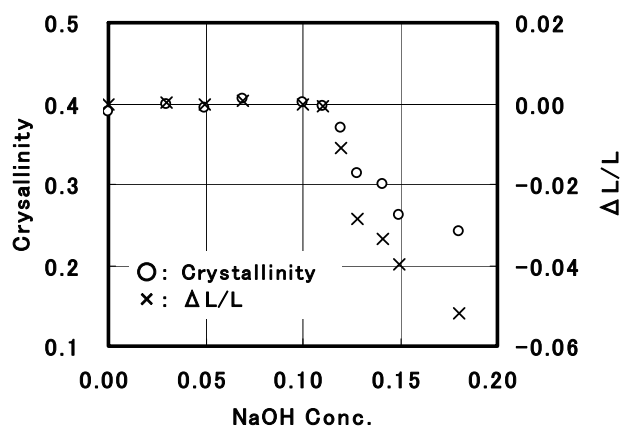
328

329

330

331

332 Figure 2



333

334

335

336

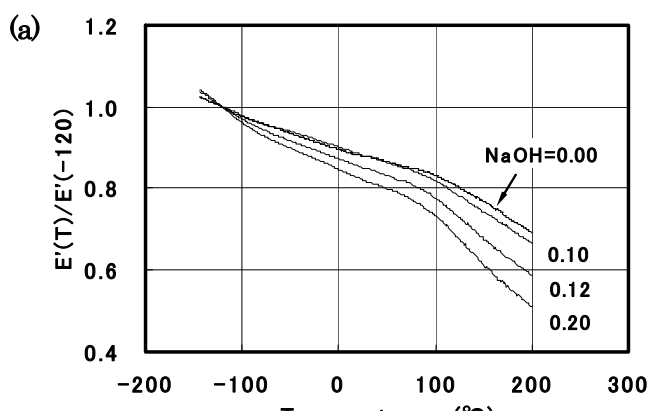
337

338

339

340

341

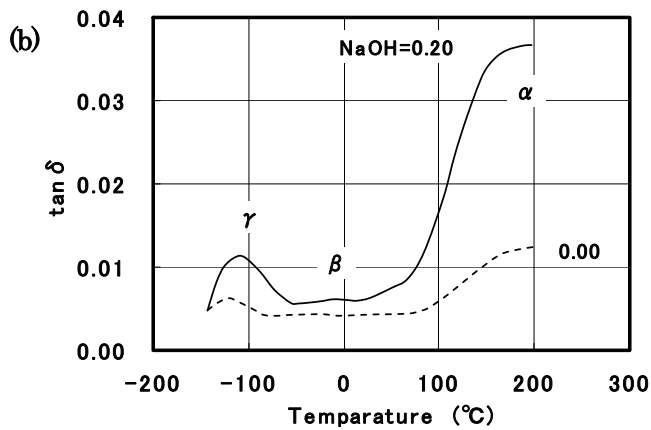


342

343

344

345



346

347 Figure 3

348

349

350

351

352

353

354

355

356

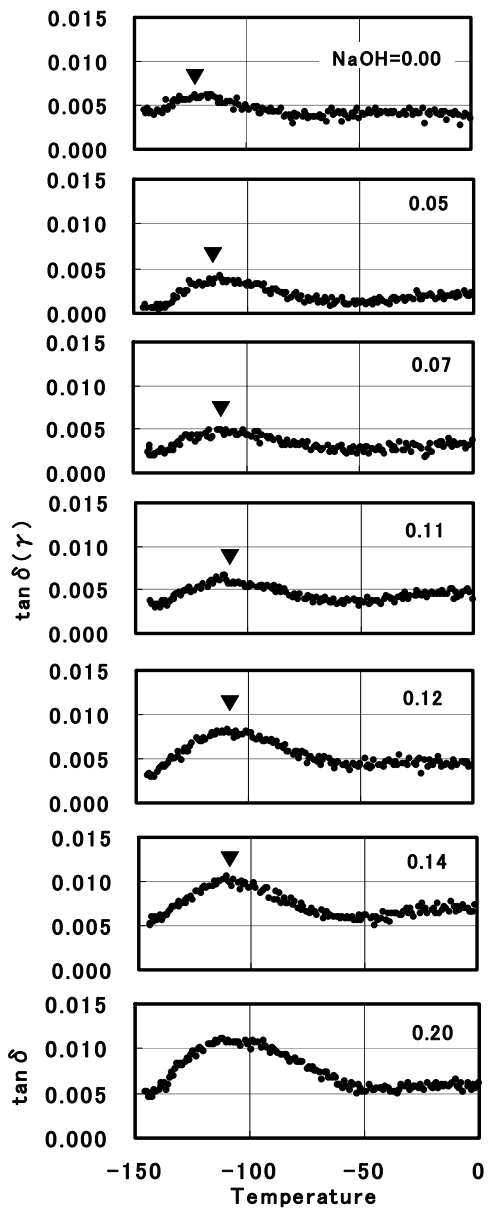
357

358

359

360

361



362 Figure 4

363

364

365

366

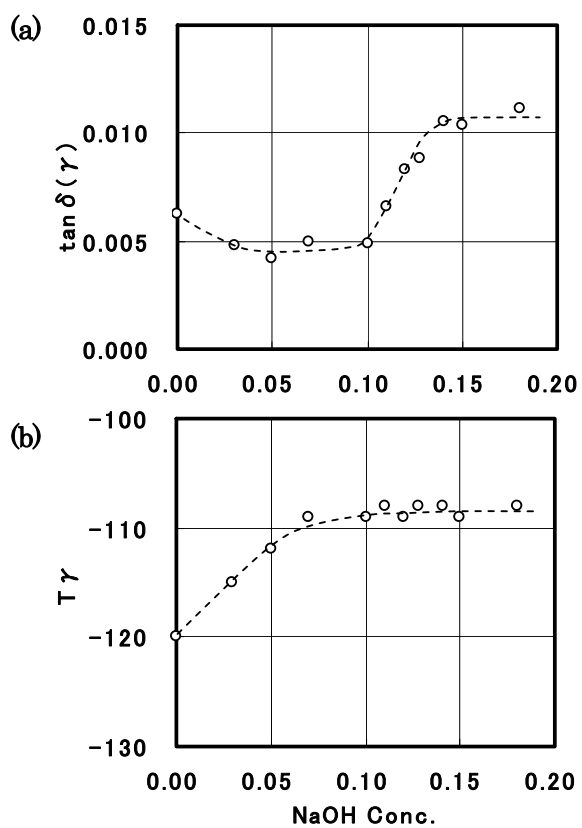
367

368

369

370

371



372

373

374

375

376

377 Figure 5

378

379

380

381

382

383

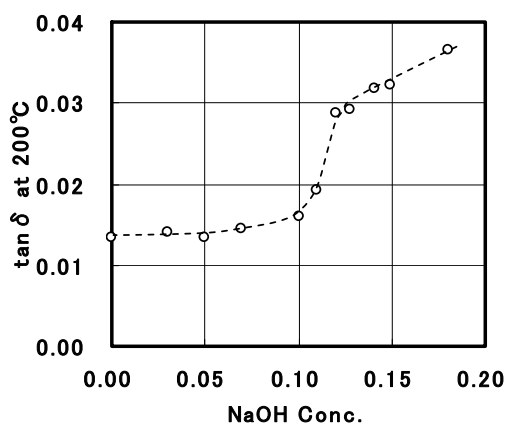
384

385

386

387

388



389 Figure 6



390

391

392

393

394

395

396

397

398

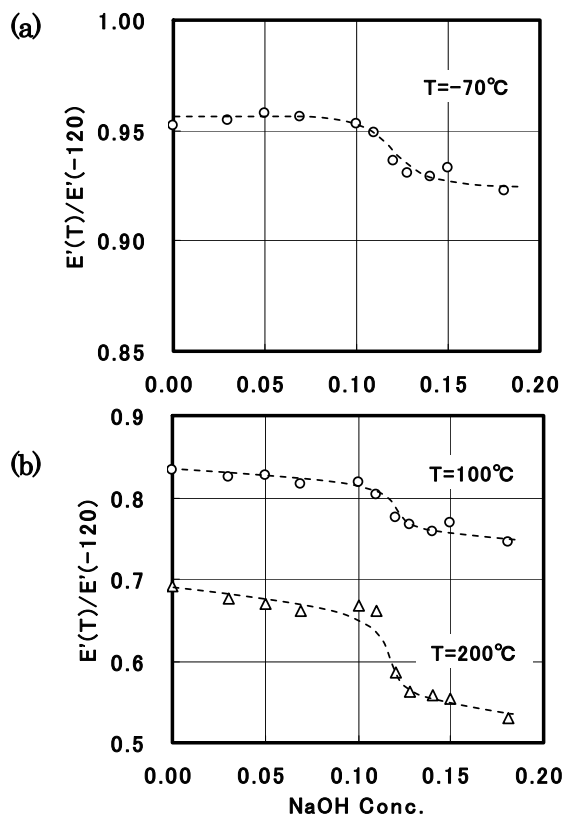
399

400

401

402

403 Figure 7



404

405

406

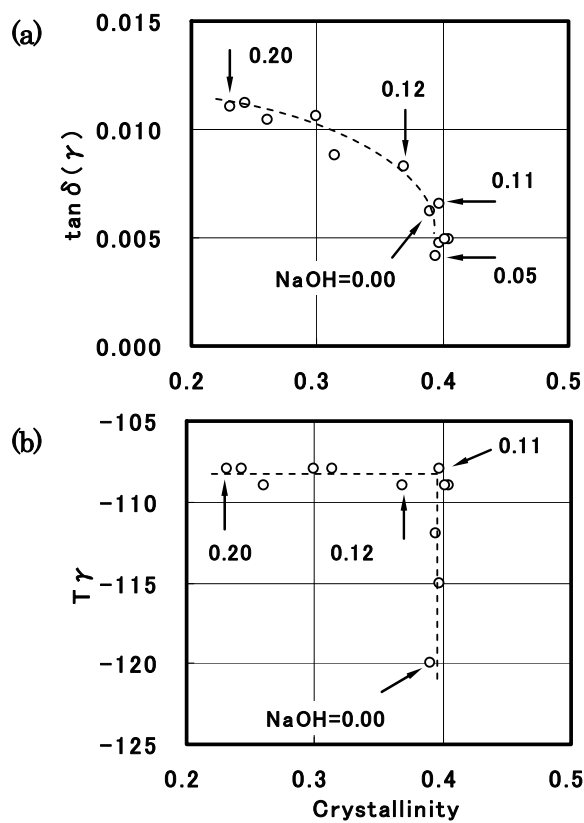
407

408

409

410

411



416

417 Figure 8

418

419

420

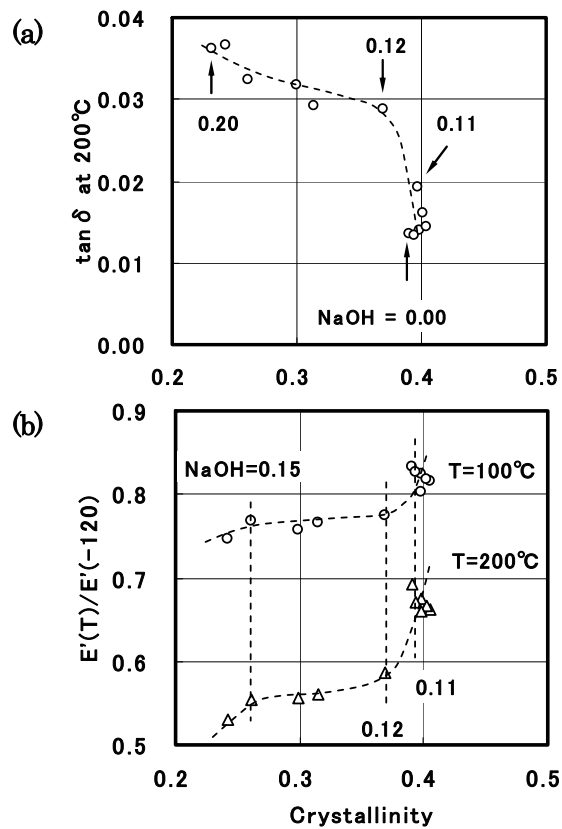
421

422

423

424

425



426

427 Figure 9

428

429

430